Accepted Manuscript

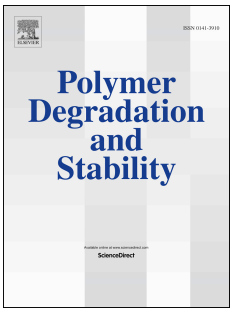

Characterization and degradation characteristics of poly(ε-caprolactone)-based composites reinforced with almond skin residues

Arantzazu Valdés García, Marina Ramos Santonja, Ana Beltrán Sanahuja, María del Carmen Garrigós Selva

PII: S0141-3910(14)00093-7

DOI: 10.1016/j.polymdegradstab.2014.03.011

Reference: PDST 7272

To appear in: *Polymer Degradation and Stability*

Received Date: 8 December 2013

Revised Date: 12 February 2014

Accepted Date: 4 March 2014

Please cite this article as: García AV, Santonja MR, Sanahuja AB, Selva MdCG, Characterization and degradation characteristics of poly(ε-caprolactone)-based composites reinforced with almond skin residues, *Polymer Degradation and Stability* (2014), doi: 10.1016/j.polymdegradstab.2014.03.011.

Characterization and degradation characteristics of poly(ε-caprolactone)-based composites reinforced with almond skin residues.

Arantzazu Valdés García*, Marina Ramos Santonja, Ana Beltrán Sanahuja, María del Carmen Garrigós Selva.

Analytical Chemistry, Nutrition & Food Sciences Department, University of Alicante, 03080, Alicante, Spain.

*All correspondence should be addressed to this author:

Arantzazu Valdés García

Analytical Chemistry, Nutrition & Food Sciences Department, University of Alicante, 03080, Alicante, Spain.

Tel: +34 965903400. Ext 1187. Fax: +34 965903527.

E-mail: arancha.valdes@ua.es

ABSTRACT

Poly(ε-caprolactone), PCL, degradation by microorganisms is a very interesting feature for its potential use in massive applications, such as food packaging. Blends of PCL with natural fibres, such as those from agricultural and food processing wastes, have proved effective by permitting a substantial reduction of the material costs, but also playing a role as reinforcement in mechanical properties. This study is focused on the evaluation of morphological, mechanical, thermal, barrier properties and degradation in composting environment of new bio-composites based on PCL and almond skin (AS) filler at different contents (0, 10, 20 and 30 wt%). Results showed a clear improvement in mechanical properties, corresponding to a gain in elastic modulus of 17% at 10 wt% particle loading. Lower melting and crystallization enthalpies and higher crystallinity values were obtained for bio-composites compared with neat PCL. Some decrease in thermal stability and increase in oxygen and water vapour barrier properties were also observed for composites with increasing filler content. PCL/AS composites showed higher biodegradability than pure PCL, which can be explained in terms of the depressed crystallization enthalpy of the polymer matrix and improved hydrophilicity. PCL-based composites reinforced with almond skin filler at 10 wt% loading have shown as promising environmentally-friendly materials for food packaging showing a high disintegration rate, increasing the added-value potential of agricultural wastes and reducing the packaging cost.

Keywords: Bio-composites, Degradation, Poly(ε-caprolactone), Almond skin, Reinforcement.

1. Introduction

Nowadays there is a growing interest in the development of biodegradable polymers to reduce the dependence on fossil fuels and to change to sustainable materials. Poly(ε-caprolactone), PCL, is a biodegradable semicrystalline and linear aliphatic polyester produced by chemical synthesis from crude oil via the ring opening polymerization of caprolactone monomer. PCL has shown degradation by the action of aerobic and anaerobic microorganisms that are widely distributed in various ecosystems, being its biodegradation very slow and leading to the formation of carbon dioxide, water, methane, biomass and mineral salts [1-3]. However, large-scale application of PCL has been limited because of its relative high price (ranging 4.50-6.00 € per kg) [4], as well as some intrinsic inferior properties [5].

PCL is one of the most widely studied biopolymers and has FDA approval in various devices for medical applications [6]. The use of PCL for food packaging applications has been recently reported by several authors, since the main commercial application of PCL is in the manufacture of biodegradable bottles and compostable bags [7]. In this sense, Martinez et al. suggested that the combination of cold storage with PCL incorporating ciannamaldehyde, as a natural biocide agent, could be suitable for the controlled diffusion of this agent extending the shelf-life of packaged food products [8]. Antimicrobial PCL nanocomposites with thymol were also developed by Sánchez et al [9]. On the other hand, Pérez et al. [10] developed an interesting storage system for refrigeration by using PCL and encapsulated dodecane obtaining coating materials with energy storage capacity. Blends of chitosan and PCL were studied by Swapna et al. showing good tensile strength and low water vapour permeability, for the potential application in fruits and vegetables packaging to extended their storage life [11].

Ludueña et al. also studied PCL with different lignocellulosic fillers for food packaging applications [12].

Blending PCL with other materials, such as natural fibres, has proved to be an effective method to reduce the final price of the material and enhance the biodegradability of the resulting composites. Natural fibres also act as reinforcement by improving mechanical properties, expanding the application areas of the obtained composites. The main advantages of such fibres are their good mechanical performance, low cost, renewability and biodegradability [12]. In general, natural fibres are suitable for reinforcing plastics due to their relatively high strength, stiffness and low density [13]. Agricultural by-products are alternative lignocellulosic materials, which are produced in large quantities every year [5]. Different types of cellulose based natural fibres and agricultural by-products (such as wood fibre [3]; agricultural cotton, cellulose and hydrolyzed-cellulose [12]; flax and rami fibres [14,15]; nanocrystalline cellulose from bleached softwood kraft pulp [7]; rice husk; abaca fibres; wood flour, lignin and wheat gluten [16]) have been successfully incorporated as fillers into PCL to obtain biodegradable composites.

Almond (*Prunus amygdalus L.*) is an important crop cultivated in countries such as USA, Spain, Morocco, Iran and Turkey, with a worldwide production about 2.3 million tones in 2009 [17]. Industrial processing of almonds starts with the removal of the external coating, with the skin contributing to around 6.0-8.4 % of the seed [18]. This biodegradable residue is considered to have one of the highest fibre contents of all edible nuts (around 12%), among other interesting compounds such as flavonoids and phenolic acids with high antioxidant activity [19]. The percentage of by-products obtained from industrial processing of almonds is consequently very high and industries are forced to consider ways of treating or using them. Up to now, the application of

these agricultural residues has not received enough attention, causing potential disposal problems; and most of them are just incinerated or dumped without control causing several environmental problems [20] or used as animal feeds [5]. For this reason, the incorporation of low-cost almond skin (AS) residues into a biodegradable polymer (such as PCL) is an attractive alternative to transform agricultural residues into useful industrial resources, with a positive benefit on environment, energy and economy.

The research on almond reinforced composites from the literature is not very extensive and it is limited to the use of almond shell as filler. Pirayesh and col. studied the suitability of using almond and walnut/almond shells in wood-based composite manufacturing, significantly reducing the formaldehyde emissions as well as highly improving water resistance of the panels [21,22]. Regarding polymer-based composites, Gürü et al. used almond shells as a filler material for urea-formaldehyde-based composites [23]. Finally, almond shells particles were used as reinforcement in a thermoplastic matrix as polypropylene, with and without different compatibilizers, by using various particle contents up to 30 wt% [24]; obtaining a clear improvement in mechanical and rheological properties.

To the best of our knowledge, there is no information in the literature on using almond skin (AS) in the production of PCL bio-composites. Therefore, the aim of this work is the development and characterization of novel PCL/AS bio-composites with different AS residue contents (0, 10, 20 and 30 wt%), giving some added-value to agricultural wastes. Special effort will be focused in evaluating the effect of the filler addition on the morphological, mechanical, thermal, barrier properties and the degradation behaviour in composting conditions of the obtained bio-composites. All these properties are relevant aspects for packaging applications.

2. Experimental

2.1. Materials

Poly(ε-caprolactone) (PCL, CAPA®6800) commercial grade (pellets, Mn = 80.000, density = 1.1g cm^{-3}) was kindly supplied by Perstorp Holding AB (Sweden).

Almond skins used as filler were supplied by "Almendras Llopis" (Alicante, Spain) as an industrial by-product. They were grounded with a high speed rotor mill (Ultra Centrifugal Mill ZM 200, RETSCH, Haan, Germany) equipped with a 1 mm sieve size. The AS fraction obtained was then dried in a laboratory oven at 100 °C for 24 h to moisture content of 0-1 %. The particle size of the resulting AS filler was determined by optical microscopy at 50x magnification with a mean diameter of 50 µm.

2.2. Bio-composites preparation

PCL/AS composites were processed by melt blending in a Haake Polylab QC mixer (ThermoFischer Scientific, Waltham, MA, USA) at 80 ºC for 5 min at 100 rpm. Before processing, PCL was left in an oven at 50 ºC for 20 h to eliminate moisture. Four different formulations were obtained by adding to the polymer different AS filler contents (0, 10, 20 and 30 wt%). The 50 cm^3 mixing chamber was filled with 50 g total mass.

Films were obtained by compression-moulding at 120 ºC in a hot-plate hydraulic press (Carver Inc, Model 3850, USA). Materials were kept between the plates at atmospheric pressure for 5 min until melting and then they were successively pressed under 2 MPa (1 min), 3 MPa (1 min) and finally 5 MPa (5 min) to liberate the trapped air bubbles. The average thickness of the obtained films was 210 ± 1 µm measured with a 293 MDC-Lite Digimatic Micrometer (Mitutoyo, Japan) at five random positions, after 48 h of conditioning at 50 % relative humidity (RH) and 23 ºC. The obtained

150 composite films were named as PCL, PCL10%, PCL20% and PCL30%; where the
151 number is the percentage filler content by weight.
152
153 2.3. Bio-composites characterization
154 2.3.1. Morphological analysis
155 The cryo-fractured surfaces of bio-composite films were analyzed by using a
156 JEOL JSM-840 scanning electron microscope (Peabody, MA, USA) under an
157 acceleration voltage of 15 kV. Samples were coated with gold under vacuum using a
158 SCD 004 Balzers sputter coater (Bal Tec. AG, Fürstentum, Lichtenstein) prior to
159 scanning in order to increase their electrical conductivity. Images were registered at
160 magnifications 500x in order to study the filler dispersion.
161
162 2.3.2. Attenuated total reflectance infrared spectroscopy (ATR-FTIR)
163 ATR-FTIR spectra were collected by using a Bruker Analitik IFS 66 FTIR
164 spectrometer (Ettlingen, Germany) equipped with a DTGS KBr detector, a Golden Gate
165 Single Reflection Diamond ATR accessory (incident angle of 45º), and OPUS 3.1 data
166 collection software program. Films (1×1 mm^2) were directly placed on the ATR crystal
167 area. Spectra were recorded in the absorbance mode from 4.000 to 600 cm^{-1}, using 64
168 scans and 4 cm^{-1} resolution, and corrected against the background spectrum of air. Two
169 spectra replicates were obtained for each sample.
170
171 2.3.3. Mechanical properties
172 Tensile tests were performed using a 3340 Series Single Column System Instron
173 Instrument, LR30K model (Fareham Hants, UK) equipped with a 2 kN load cell. Tests
174 were performed in rectangular probes (100 x 10 mm^2), an initial grip separation of 60

mm and crosshead speed of 25 mm min^{-1}. Before testing, all samples were equilibrated for 48 h at 50 % RH. Percentage elongation at break and elastic modulus were calculated from the resulting stress-strain curves according to ASTM D882-09 standard [25]. Tests were carried out at room temperature. Five repetitions were performed for each film composition, and mean values were reported.

2.3.4. Barrier properties

Water absorption by bio-composite films was determined in triplicate according to UNE-EN ISO 62:2008 standard [26]. Samples (8 cm lengh x 1 cm width x 4 mm thick) were dried in a vacuum oven at 23 ºC for 4 h, cooled in a desiccator, and then immediately weighed to the nearest 0.001 g. Thereafter, samples were immersed in distilled water and maintained at 23 ºC and 50 % RH. Finally, samples were taken out at different times, wiped out properly and then reweighed. Water absorption was calculated according to the formula:

$$(W_t - W_0)/W_t \times 100\% \quad (1)$$

where W_0 was the sample weight prior to water adsorption experiment and W_t was the final mass at the pre-determined time t.

Water vapour permeability (WVP) was determined in triplicate according to UNE 53097:2002 standard [27] by using the Desiccant Method ($CaCl_2$). Samples of 95 mm diameter were fixed with paraffin on the top of aluminium capsules containing $CaCl_2$, and they were placed in a climate chamber (Dycometal, Barcelona, Spain) at 20.0 ± 0.1 ºC and 50 ± 2 % RH. Capsules were periodically weighed until the steady state was reached and no significant changes in mass were noticed.

Oxygen transmission rate (OTR) tests were carried out with an oxygen permeation analyzer (8500 model Systech Instruments, Metrotec S.A, Spain). Bio-

composite films were cut into 14-cm diameter circles for each formulation and they were clamped in the diffusion chamber at 25 ± 1 ºC. Tests were carried out by introducing O_2 (99.9% purity) into the upper half of the diffusion chamber while N_2 was injected into the lower half, where an oxygen sensor was located. Tests were performed in triplicate and were expressed as oxygen transmission rate per film thickness (OTR·e).

2.3.5. Thermal properties

Differential scanning calorimetry (DSC) tests were conducted in triplicate by using a TA DSC Q-2000 instrument (New Castle, DE, USA) under inert N_2 atmosphere (50 mL min^{-1}). Films (3.0 ± 0.1 mg) were introduced in aluminium pans and were submitted to the following thermal program: heating from -80 ºC to 160 ºC (3 min hold), cooling to -80 ºC (3 min hold) and heating to 160 ºC, all steps at 10 ºC min^{-1}. Calorimetric curves were analysed using the Universal Analysis TM Software (TA Instruments, New Castle, DE) to obtain crystallization and melting parameters which were determined from the second heating scan. The degree of crystallinity (χ_c) of each material was calculated by equation (2):

$$Xc = \frac{\Delta Hm}{w * \Delta H^{\circ}m} * 100 \quad (2)$$

where ΔH_m is the experimental melting enthalpy of the sample, w is the PCL weight fraction in the bio-composite film and ΔH_m^{o} is the melting enthalpy of 100 % crystalline PCL (136 J g^{-1}) [12].

Thermogravimetric analysis (TGA) was performed in a TGA/SDTA 851 Mettler Toledo (Schwarzenbach, Switzerland) thermal analyzer. Films (4.0 ± 0.1 mg) were weighed in alumina pans and were heated from 30 ºC to 700 ºC at 10 ºC min^{-1} under N_2 atmosphere (50 mL min^{-1}). Analyses were performed in triplicate and two parameters were determined: initial degradation temperature, T_i (ºC), calculated at 5 % of weight

loss; and temperature of maximum degradation, T_{max} (ºC), corresponding to the maximum decomposition rate.

2.3.6. Disintegration tests

Disintegration tests in composting conditions were carried out as reported by Ludeña et al. and following ISO 20200 standard method using commercial compost with certain amount of sawdust, rabbit food, starch, oil and urea [12,28]. Tested samples were obtained from the previously prepared films, which were cut in square pieces (15 x 15 x 0.2 mm^3), buried at 5 cm depth in perforated boxes and incubated at 25 ºC. The aerobic conditions were guaranteed by mixing the compost softly and by the periodical addition of water according to the standard requirements.

After disintegration experiments (0, 7, 10, 15, 30, 45, 60 and 75 days), samples were removed from the compost and immediately washed with distilled water to remove traces of compost extracted from the container and to stop any further microbial reaction. Then, samples were dried at 23 ºC and 50 % RH for 24 h before gravimetrical analysis. The disintegrability value for each burial sample was obtained by using equation (3):

$$Disintegrability\ (\%) = [(w_0 - w_t)/w_0] \cdot 100 \quad (3)$$

where w_0 is the initial mass and w_t is the remaining mass at different stages of incubation. All results are the average of two replicates.

Evaluation of degradation was completed by taking photographs of samples for visual evaluation of physical alterations with disintegration time. DSC tests, as previously described in section 2.3.5, were used in order to establish changes in the structure of the degraded composite films.

2.4. Statistical analysis

Statistical analysis of results was performed with SPSS commercial software (Version 15.0, Chicago, IL). A one-way analysis of variance (ANOVA) was carried out. Differences between means were assessed on the basis of confidence intervals using the Tukey test at a $p \leq 0.05$ significance level.

3. Results and discussion

3.1. Morphological analysis

The surface morphology of neat PCL and PCL/AS composite films was studied by scanning electron microscopy (Fig. 1). As it can be seen, regions with dispersed filler and some others with agglomerates were observed, being more evident in PCL with 30 wt%. As a result, the dispersion of AS particles inside the PCL matrix was less efficient for the higher weight fraction samples, such as 20 and 30 wt% formulations. Similar results were reported by Ludueña et al. for PCL based composites containing different lignocellulosic filler types and contents [12]. This fact could be attributed to the high hydrophilicity of the filler, and hence poor polymer/filler compatibility since PCL is strongly hydrophobic; as well as to the incremented filler exposed surface area that promotes the formation of hydrogen bonds between the individual hydrophilic fibres.

3.2. Attenuated total reflectance infrared spectroscopy (ATR-FTIR)

Fig. 2 shows the ATR-FTIR spectra obtained for neat PCL and PCL30% composite. The observed features are characteristic of PCL polymer and similar results have been reported by other authors [29,30]. Table 1 shows the average of the main significant bands observed for each sample in the spectra.

Significant differences were observed between neat PCL and the obtained bio-composite films as a result of the addition of the AS residue regarding the wavenumber

and maximum absorbance values of the wide band appearing at 3400 cm^{-1} which is characteristic of the O-H bonds ($p < 0.05$). As a result, a significant increase in absorbance was obtained for this band with increasing AS weight fraction in the formulations ($p < 0.05$). This band is characteristic of the AS residue spectrum (Fig. 2.b), and it could be related with stretching vibrations of the hydroxyl groups of carbohydrates such as glucose, galactose and manose as major components present in AS [19,24]; which are formed by carbon, hydrogen and oxygen with general formula $(CH_2O)_n$.

In addition, statistical significant differences between neat PCL and bio-composites were observed regarding the wavenumber value of the band observed at 2940-2870 cm^{-1} ($p < 0.05$) (Fig. 2.c). In this case, as filler content increased, the intensity of the band observed at 2943 cm^{-1} tended to decreased. This fact could be due to a lower PCL content in the composites [29].

Significant differences between samples were also found regarding the peak at 1724 cm^{-1} due to the C=O bonding [31]. In this sense, the increment of AS content in the bio-composites is expected to increase the attached C=O functional groups while decreasing the free ones, which are related to the decrease in the band intensity observed at 1724 cm^{-1} (Fig. 2.d) [31,32]. Finally, the absorbance of the bands corresponding to the C–O lactones stretching (1180 cm^{-1}), and C-O-C stretching (1045 cm^{-1}) also decreased when polymer content was reduced [31,32].

3.3. Mechanical properties

The incorporation of AS particles clearly influenced the mechanical properties of pure PCL matrix with increasing weight fraction (Table 2). As a result, a significant increase in the elastic modulus of these samples was observed with the addition of the

almond residue ($p < 0.05$) for PCL10% and PCL20%. This fact is due to the high tensile modulus of particles compared with neat PCL and indicates that the rigidity of the material increased with the addition of the filler [24]. The highest elastic modulus value was obtained at 10% loading, in contrast with PCL30% which showed lower value than neat PCL. These results are in agreement with the filler dispersion inside the matrix previously analyzed by SEM; where higher filler dispersion and better adhesion between AS residue and PCL matrix was observed for PCL10% whereas some agglomeration of the filler takes place for PCL30% (Fig. 1).

The incorporation of the filler also drives to a significant decrease in the elongation at break with increasing AS content ($p < 0.05$). As it can be seen (Table 2), all bio-composite films containing the AS residue showed lower values of elongation at break than neat PCL, obtaining the lowest value at 30% loading. The decreased in elongation at break values may be related to the increased stiffness of composite films by the addition of the AS residue because the fibre restricted the polymer chain elongation [33-35]. The elongation at break is affected by the volume fraction of the added reinforcement, the dispersion in the matrix and the interaction between the reinforcement and the matrix [36]. The effectiveness of composites material largely depends on their ability to transfer stress from the polymer matrix (continuous phase) to fillers (dispersed phase) [24]. In this sense, low interactions between filler and matrix are responsible for an effect of stress concentration, and they generate the beginning of the fracture [37]. The decrease in of elongation at break with the addition of fibres is commonly observed in thermoplastic composites, where the addition of stiff reinforcements causes stress concentrations [36]. In this case, higher AS loading in PCL composite films results in poor compatibility between phases, in agreeement with the obtained SEM results, causing substantial local stress concentrations, accelerating

failure and sample break. Similar results were obtained by Ludueña et al. when studying the mechanical behaviour of PCL composites containing different lignocellulosic fillers at different concentrations [12].

These results clearly suggest that AS residues could act as reinforcement agents in PCL composite films at 10 wt% loading [34]. In general, the mechanical properties of fibres-polymer composites are a consequence of the combination of different parameters: particle size, highest or lowest chemical compatibility, interfacial strength, filler dispersion and filler aspect ratio and particle loading [12,24].

3.4. Barrier properties.

Results obtained for oxygen transmission rate per film thickness (*e*), OTR•*e*, for PCL and PCL/AS composite films are shown in Table 2. As it can be seen, bio-composite films containing AS showed significant higher OTR·*e* values ($p < 0.05$) compared with neat PCL. No significant differences were observed by comparing OTR•*e* results for films containing 10 and 20 wt% of filler ($p > 0.05$). However, PCL30% films showed a great increase in OTR·*e* values suggesting a possible filler agglomeration in films with higher fibre loading; as it was already observed by SEM.

Table 2 also shows the WVP values obtained for PCL and PCL/AS composites. Slightly higher values were observed for PCL20% and PCL30% formulations compared to the neat matrix ($p < 0.05$). However, no significant differences were found for neat PCL and PCL10% composite ($p > 0.05$). In general, results observed for OTR and WVP values increased with the filler content, which can be attributed to agglomeration causing a reduction in the matrix homogeneity and cohesion and leading to preferential penetrant paths and to detrimental effects in barrier properties [38].

When considering barrier properties, a balance between different mechanisms has been reported to be responsible of the final behaviour of composites [12]: (1) the crystallinity degree of the matrix goes down by the presence of the filler, making the matrix more permeable to water or oxygen molecules; (2) the presence of the filler increases the tortuosity of the pathway for water or oxygen molecules to pass through the film; (3) weak interfacial strength and agglomeration of the filler promotes the generation of voids in the polymer/filler interface making easier the transport of the water or oxygen molecules through these regions.

Regarding water absorption, Fig. 3 compares the curves obtained for neat PCL and PCL/AS composites at 23 ºC and 50 % RH. As it was expected, higher water absorption values for samples with increased AS residue contents were obtained, showing the neat matrix the lowest value. Water absorption largely depends on the hygroscopic components present in the biocomposite; so, if the polymer matrix is hydrophobic it may act as a semipermeable membrane. Moisture penetration into composite materials has been reported to be conducted by three different mechanisms: (1) diffusion of water molecules inside the microgaps between polymer chains and natural fillers; (2) capillary transport into the gaps and flaws at the interfaces between fibres and polymer because of incomplete wettability and impregnation; (3) transport through microcracks in the matrix, formed during the compounding process. Accordingly, water absorption in biocomposites can be influenced by several factors, such as fibre loading (higher fibre content should contribute to higher moisture absorption), the chemical nature of lignocellulosic fillers, fibre geometry, and, especially, the compatibilization between matrix and fillers (improved interfacial adhesion would result in fewer and smaller microgaps where water uptake may occur) [1].

375

376 3.5. Thermal properties

377 3.5.1. DSC analysis

378 Fig. 4 shows the thermograms, corresponding to the second heating scan, of neat
379 PCL and PCL/AS composites. All materials exhibited two energy transitions: an
380 exothermic crystallization around 30 °C and an endothermic melting at approximately
381 55 °C, characteristics of PCL by its semi-crystalline structure. A significant decrease in
382 melting parameters (temperature and enthalpy) ($p < 0.05$) was observed for PCL30%
383 (Table 3). In this sense, the incorporation of the AS residue can restrict the periodic
384 arrangements of PCL chains into its lattice, leading to some loss in the polymer
385 crystallinity in bio-composites than in neat PCL, resulting in decreased melting
386 parameters [5]. Regarding crystallization parameters, the observed decrease in ΔH_c and
387 increase in T_c in PCL30% (Table 3) ($p < 0.05$) suggested a decrease on the extent and
388 crystallization kinetics of PCL upon heating, probably due to highly restricted
389 segmental motions at the organic–inorganic interface. Indeed, the glass transition
390 temperature (T_g) of this material increased about 5 ºC (Table 3), thus confirming the
391 occurrence of restricted polymer chain movements after the addition of AS particles
392 [39]. These results are in agreement with those reported in a previous work when
393 studying the effect of cellulose nanocrystals incorporation obtained by acid hydrolysis
394 of Luffa cylindrica fibres as reinforcing phase in PCL nano-biocomposites. In this
395 sense, it was suggested that T_g values displacement could be related to the restriction of
396 the rotational backbone motions of PCL polymer chains through the establishment of
397 hydrogen bonding forces between individual fibres into the polymer matrix [32].

398 Finally, the crystallinity degree obtained for all materials are also shown in Table
399 3. Previous studies demonstrated that PCL is a partial crystalline polyester with

crystallinity between 40–60% [5]. As it can be seen from Table 3, the crystallinity of the PCL/AS composites increased at higher AS loading. These results are consistent with those found by Chun et al. when studying cocoa pod husk-filled polypropylene composites and this behaviour is due to the nucleating effect of the AS residue modifying the crystallisation by increasing the number of nucleating sites [40]. For PCL30% this phenomena could be restricted in some extent by filler agglomeration with reduces the filler exposed surface area [12].

3.5.2. Thermal stability (TGA)

The thermal stability of the AS residue was studied by TGA. The DTG curve obtained for AS particles (Fig. 5) showed an initial step between 40 and 150 ºC as the result of the loss of volatile compounds and water [41]. Three main thermal degradation peaks were observed. A similar DTG profile was observed by Essabir et al. when studying the thermal stability of almond shells particles used as reinforcement in polypropylene matrices. The first peak observed between 285 ºC and 320 ºC was attributed to the thermal depolymerisation of hemicelluloses, and the second peak which occurs in the 320–400 ºC range corresponded to the cellulose degradation. Finally, the third stage is associated to the degradation of lignin at 420 ºC, which occurs slowly in the temperature range due to its complex structure [24].

In the case of PCL, thermal degradation in inert atmosphere takes place through the rupture of the polyester chains via ester pyrolysis reaction with the release of CO_2, H_2O and formation of carboxylic acid groups. Pyrolysis provokes chain cleavages randomly distributed along the chain and when two pyrolysis reactions occur with neighbouring ester functions, one of the reaction products is 5-hexenoic acid [39].

Fig. 5 also shows DTG curves obtained for neat PCL and PCL/AS in nitrogen. As it can be seen, at low filler contents (10 wt%) the thermal stability of the PCL matrix was not significantly affected by the presence of the filler, showing initial and maximum degradation temperatures around 385 and 415 ºC, respectively (Table 3). However, since filler loading increased some extra peaks related to the thermal degradation of the AS residues were observed, being more evident for the PCL30% film. This behaviour is related to the lower matrix homogeneity of this formulation. Similar results were obtained by Ludueña et al. for the incorporation of some lignocellulosic fillers into PCL at different concentrations [12]. As a result, some decrease in thermal stability was observed for PCL20% and PCL30% composites regarding T_{ini} and T_{max} values (Table 3).

In conclusion, the addition of AS particles to the polymer matrix at 20 and 30 wt% may promote earlier degradation of the overall material. This behaviour was also reported by Jiménez et al. when preparing mixtures based on PCL with different natural fillers; since they found that the early formation of acidic products from cellulose and hemicellulose decomposition promoted the random scission of ester linkages in a PCL matrix reinforced with sisal fibres [42,43].

3.6. Disintegration tests

The effect of the addition of natural fibres on the biodegradation process of biocomposites is an active topic of research. In general, the presence of lignocellulosic reinforcements enhances the microbial attack and the biodegradation rates by promoting biofouling and the adhesion of microorganisms to the surface. The kinetics of the biodegradation process depends on different factors, such as the susceptibility of the different components of the biocomposites; the interfacial adhesion by selecting the

type of natural filler that exhibits higher fibre-fibre and fibre-matrix interactions; the hydrophilic nature of the polymeric matrix; and crystallinity. In this sense, PCL biocomposites may exhibit slower biodegradation rates than other biopolymer-based composites, due to their tailored semicrystalline structure and relative hydrophobicity [1].

3.6.1. Physical alterations

The visual evaluation of physical alterations of all samples at different degradation times (0, 30 and 75 days) in composting conditions at 25 ºC is shown in Fig. 6. All samples showed considerable changes in their morphology after 30 days of the disintegration study with a general roughing and holes formation. These modifications were indicative of the beginning of the polymer hydrolytic degradation process, which was related to the moisture absorption by the polymer matrix. In this sense, the incorporation of AS residue accelerated the water intake as fibres facilitated the access of water into the PCL matrix of the bio-composite films, and the disintegration rate of PCL matrix became more pronounced with the increasing fibre contents [16]. Results obtained at longer testing times showed that physical degradation progressed with burial time resulting in the complete loss of their initial morphology and general fragmentation after 75 days.

Fig. 7 shows the evolution of the disintegrability (%) as function of time for neat PCL and PCL/AS composites in composting conditions. Before 15 days of treatment, no significant differences were observed between all samples, showing a similar weight loss ($p > 0.05$). However, significant differences between neat PCL and the rest of bio-composites were observed after 15 testing days ($p < 0.05$). These differences could be related to the presence of the fibre which can produce strong interactions during the

initial period due to the formation of H-bonds, producing a physical network which prevents the water uptake, and thus reducing the accessibility to soil microflora [35]. In this sense, the diffusivity of water is strongly influenced by the material's microstructure as well as porosity and water affinity of the polymer components. These kind of interactions between cellulose fibres and polymer matrices were reported by Dufresne et al. [44,45] for systems composed by thermoplastic starch and microfibrils obtained from potato pulp, observing a decrease in water uptake by increasing the cellulose contents. This phenomenon was ascribed to the formation of a microfibril network, which prevented the swelling of the biocomposite and water absorption.

The end of the disintegration study was 75 days, when PCL/AS bio-composites were considered to be totally disintegrated, according to the ISO 20200 standard requirements [28], which states 90 % disintegration for a biodegradable material. At that time, bio-composites containing 10-30 wt% of AS showed higher disintegration values that neat PCL. In this sense, it was reported that the addition of natural fillers, such as rice husk fibres, into PCL increased the disintegration rate as they could facilitate the access of water into the polymer matrix [16]; as water absorption tests have shown in this study. A similar tendency was also observed by other researchers for neat PCL and PCL-based composites in natural media, such as soil [5,12,37].

According to Fukushima, et al. [46] the main mechanism of PCL degradation involves the scission of PCL ester bonds by enzyme-catalyzed hydrolysis due to microorganisms present in the compost with the formation of alcohol and carboxylic acid groups, as shown in Scheme 4.

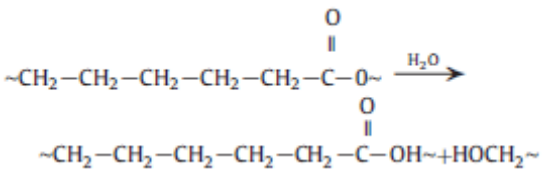

(4)

PCL degradation proceeds in two stages: random hydrolytic ester cleavage and weight loss through the diffusion of oligomeric species from the bulk [47]. Then, the biodegradation process is dependent on the water bio-availability that promotes the microbial attack and the matrix hydrolysis. PCL exhibits high hydrophobicity, which can inhibit the access of water to the polymer matrix during the degradation, and thus retard the hydrolysis of ester bonds. The hydrophobicity of poly(ε-caprolactone) could lead to surface erosion/degradation [47]. In contrast, AS is highly hydrophilic due to the structure with multiple hydroxyl groups of carbohydrates. Therefore, the incorporation of the AS can facilitate the access of water to the PCL matrix, leading to accelerated degradation. Due to the natural origin of the AS, its presence can favour the enzymes binding onto the material surface, thereby promoting the degradation of the neighbouring PCL matrix [5]. Both effects are expected to be enhanced with increasing AS loading.

The following characteristics of these fibres and their effect on the properties of the polymer matrix have been reported to simultaneously affect the biodegradation process of the composites [12]:

(1) The high hydrophilicity of natural fibres promotes the water intake and provides a rougher support for microbial growth. Then, the presence of microorganisms in soil, which are relatively active in hemicelluloses under suitable temperature and humidity conditions, could accelerate the degradation process [35]. In later stages, cellulose chains breakdown may contribute to the higher weight loss suffered by the bio-composites.

(2) Fibre agglomerates can form micro-cavities promoting the water uptake, but also drastically diminish the contact surface between the fibre and the polymer diminishing the effect mentioned in Section (1).

522

523 3.6.2. Thermal analysis (DSC)

524 Fig. 8 shows the thermograms obtained for neat PCL and PCL/AS composites
525 corresponding to the second heating after 0, 15, 30 and 75 days of degradation in
526 compost. After 15 days, as the filler content increased composites showed a
527 considerable decrease in crystallization and melting enthalpies as the consequence of
528 the formation of less perfect crystals due to polymer chain scission during the hydrolytic
529 degradation [39]; being more noticeable for PCL20% and PCL30% after 30 days as
530 these energy transitions were no longer visible. These results are consistent with the
531 high extent of polymer degradation evidenced by the visual observations and
532 disintegrability analysis. They are probably related to the scission of polymer chains
533 preventing the formation of stable crystalline structure and to the mixing upon heating
534 of PCL with the enzymes secreted by microorganisms from compost (amorphous
535 macromolecules) [39]. No significant differences were observed in crystallization and
536 melting enthalpy values for neat PCL after 75 days, indicating the lower extent of
537 polymer degradation when compared to PCL/AS composites, in particular at high filler
538 loading. This was expected for a semicrystalline polymer such as PCL, since crystalline
539 regions show the tendency to retard water uptake [47].

540 It is well known that crystallinity plays an important role in the degradation
541 behaviour of the aliphatic polyesters [5]. The observed modifications on crystallization
542 enthalpy values (ΔH_c) for PCL-AS films during biodegradation are shown in Fig. 9. No
543 significant differences in ΔH_c ($p > 0.05$) were observed for neat PCL up to 30 testing
544 days. However, PCL containing 10 wt% of AS residue did not show significant
545 differences in ΔH_c values ($p > 0.05$) up to 15 days, in contrast to 20 and 30 wt%
546 formulations which showed a significant decrease with disintegration time ($p < 0.05$). It

can be concluded that the incorporation of almond skin led to reduction in crystallinity of the polymer matrix accelerating the degradation process [12].

4. Conclusions.

Novel biodegradable composites based on poly(ε-caprolactone) (PCL) and almond skin residues (AS) were produced. A remarkable improvement in mechanical properties with the addition of AS particles was obtained indicating the potential use of this residue as reinforcement agent in PCL composites. Furthermore, the presence of AS filler accelerated the degradation of the PCL matrix in the composite films, being this effect more pronounced with the increase in AS contents. This effect was explained in terms of the reduction in crystallinity of the polymer matrix and the high hydrophilicity of the natural fibres, promoting the water uptake and, consequently, the microbial attack and hydrolysis of the PCL matrix.

The best performance regarding the studied properties was found for composite films with 10 wt% AS loading. In this sense, mechanical properties were improved with good adhesion between the AS residue and the PCL matrix, as observed by SEM. No significant differences were observed regarding thermal degradation and barrier properties compared to neat PCL. In conclusion, this formulation can be an interesting environmentally-friendly material to be used for food packaging applications showing a biodegradable nature and increasing the added-value potential of almond agricultural wastes. In this sense, it is clear that some reduction in transparency of the polymer matrix will be obtained with the AS filler incorporation, but the obtained formulation could be suitable for the development of sustainable food trays and similar containers where transparency is not an issue. Finally, an additional advantage is the reduction of the packaging cost by adding this residue.

Acknowledgements

Authors would like to thank "Almendras Llopis S.A" for kindly providing the almond skin by-product as well as to Spanish Ministry of Economy and Competitiveness for financial support (MAT-2011-28468-C02-01). Arantzazu Valdés acknowledges Conselleria de Educación (Spain) for ACIF/2010/172 Predoctoral Research Training Grant.

References

[1] Vilaplana, F, Strömberg, E, Karlsson, S. Environmental and resource aspects of sustainable biocomposites. Polymer Degradation and Stability 2010; 95: 2147-2161.

[2] Tokiwa, Y, Calabia, B, Ugwu, C, Aib, S. Biodegradability of Plastics. International Journal of Molecular Sciences 2009; 10: 3722-3742.

[3] Bikiaris, DN, Papageorgiou, GZ, Achilias, DS, Pavlidou, EZ, Stergiou, A. Miscibility and enzymatic degradation study of poly (ε-caprolactone)/poly(propylene succinate) blends. European Polymer Journal 2007; 43:2491-2503.

[4] http://www.bio-plastics.org Last access December, 2013.

[5] Zhao Q, Tao J, Yam RCM, Mok ACK, Li RKY, Song C. Biodegradation behavior of polycaprolactone/rice husk ecocomposites in simulated soil medium. Polymer Degradation and Stability 2008; 93:1571-1576.

[6] Woodruff, M., Werner, D. The return of a forgotten polymer-polycaprolactone in the 21st century. Progress in Polymer Science 2010; 35: 1217–1256.

[7] Khan, R, Beck, S, Dussault, D, Salmieri, S, Bouchard, J, Lacroix, M. Mechanical and Barrier Properties of Nanocrystalline Cellulose Reinforced Poly(caprolactone)

596 Composites: Effect of Gamma Radiation. Journal of Applied Polymer Science 2013;
597 3038-3046.
598 [8] Martínez-Abad, A., Sánchez, G., Fuster, V., Lagarón, JM. Antibacterial performance
599 of solvent cast polycaprolactone (PCL) films containing essential oils. Food Control
600 2013; 34: 214-220.
601 [9] Sánchez-García, MD., Ocio, MJ., Gimenez, E., Lagarón, JM. Novel
602 Polycaprolactone Nanocomposites Containing Thymol of Interest in Antimicrobial Film
603 and Coating Applications 2008; 24: 239-251.
604 [10] Perez-Masia, R., Lopez-Rubio, A., Fabra, MJ., Lagarón, JM. Biodegradable
605 Polyester-Based Heat Management Materials of Interest in Refrigeration and Smart
606 Packaging Coatings. Jounal of applied polymer science 2013; 130: 3251-3262.
607 [11] Swapna Joseph, C., Prashanth, H., Rastogi, NK., Indiramma, AR., Reddy, Y.,
608 Raghavarao, KSMS. Optimum Blend of Chitosan and Poly-(ε-caprolactone) for
609 Fabrication of Films for Food Packaging Applications. Food Bioprocess Technoly
610 2011; 4: 1179–1185.
611 [12] Ludueña L, Vázquez A, Alvarez V. Effect of lignocellulosic filler type and content
612 on the behavior of polycaprolactone based eco-composites for packaging applications.
613 Carbohydrate Polymers 2012; 87:411– 421.
614 [13] Faruk O, Bledzki AK, Fink H-P, Sain M. Biocomposites reinforced with natural
615 fibers: 2000–2010. Progress in Polymer Science 2012; 37:1552– 1596.
616 [14] Arbelaiz A, Fernández B, Valea A, Mondragón I. Mechanical properties of short
617 flax fibre bundle/poly(ε-caprolactone) composites: influence of matrix modification and
618 fibre content. Carbohydrate Polymers, 2006; 64:224-232.

619 [15] Xu H, Wang I, Teng C, Yu M. Biodegradable composites: ramie fibre reinforced
620 PLLA-PCL composite prepared by in situ polymerization process. Polymer Bulletin
621 2008; 61:663-670.
622 [16] Wahit MU, Akos NI, Laftah WA. Influence of Natural Fibers on the Mechanical
623 Properties and Biodegradation of Poly(lactic acid) and Poly(e-caprolactone)
624 Composites: A Review. Polymer Composites 2012; 1045-1053.
625 [17] Food and Agriculture organization of the United Nations. (FAOSTAT Database):
626 http://faostat.fao.org/ Last access November, 2013
627 [18] Garrido I, Monagas M, Gómez-Cordovés C, Bartolomé B. Polyphenols and
628 antioxidant properties of almond skins: Influence of industrial processing. Journal of
629 Food Science 2008; 73(2):106-115.
630 [19] Mandalari G, Tomaino A, Arcoraci T, Martorana M, Turco VL, Cacciola F, Rich
631 GT, Bisignano C, Saija A, Dugo P, Cross KL, Parker ML, Waldron KW, Wickham M
632 SJ. Characterization of polyphenols, lipids and dietary fibre from almond skins
633 (Amygdalus communis L.). Journal of Food Composition and Analysis 2010;
634 23(2):166-174.
635 [20] Deniz F. Dye removal by almond shell residues: Studies on biosorption
636 performance and process design. Materials Science and Engineering 2013; C 33:2821–
637 2826.
638 [21] Pirayesh H, Khazaeian A. Using almond (Prunus amygdalus L.) shell as a bio-
639 waste resource in wood based composite. Composites: Part B 2012; 43:1475–1479.
640 [22] Pirayesh H, Khanjanzadeh H, Salari A. Effect of using walnut/almond shells on
641 the physical, mechanical properties and formaldehyde emission of particleboard.
642 Composites: Part B 2013; 45:858–863.

643 [23] Gürü M, Tekeli S, Bilici I. Manufacturing of urea-formaldehyde-based composite
644 particleboard from almond shell. Materials and Design 2006; 27:1148–51.
645 [24] Essabir H, Nekhlaoui S, Malta M, Bensalah MO, Arrakhiz FZ, Qaiss A, Bouhfid R.
646 Bio-composites based on polypropylene reinforced with Almond Shells particles:
647 Mechanical and thermal properties. Materials and Design, 2013; 51:225–230.
648 [25] ASTM D882-09. Standard test method for tensile properties of thin plastic
649 sheeting. 468 Annual Book of ASTM Standards. Amer. Soc. for Testing and Materials,
650 Philadelphia, PA.
651 [26] ISO 62:2008 Plastics: Determinations of water absorption- Determination of water
652 absorbed content after immersion into water at 23 ºC.
653 [27] UNE 53097:2002 Sheet materials – Determination of water vapour transmission
654 rate – Gravimetric (dish) method.
655 [28] UNE-EN. ISO 20200:2006. Plastics - Determination of the degree of disintegration
656 of plastic materials under simulated composting conditions in a laboratory-scale test
657 (ISO 20200:2004). 2006.
658 [29] Hoidy WH, Al-Mulla EAJ, Al-Janabi KW. Mechanical and Thermal Properties of
659 PLLA/PCL Modified Clay Nanocomposites. Journal of Polymers and the Environment
660 2010; 18(4):608-616.
661 [30] Salmieri S, Lacroix M. Physicochemical Properties of Alginate/Polycaprolactone-
662 Based Films Containing Essential Oils. Journal of Agricultural and Food Chemistry
663 2006; 54:10205-102014.
664 [31] Sadeghi M, Mehdi Talakesh M, Ghalei B, Shafiei M. Preparation, characterization
665 and gas permeation properties of a polycaprolactone based polyurethane-silica
666 nanocomposite membrane. Journal of Membrane Science 2013; 427(0):21-29.

667 [32] Siqueira G, Brasa J, Follain N, Belbekhouche S, Marais S, Dufresnea A. Thermal
668 and mechanical properties of bio-nanocomposites reinforced by Luffa cylindrica
669 cellulose nanocrystals. Carbohydrate Polymers, 2013; 91:711– 717.
670 [33] Reixach R, Espinach F, Franco-Marqués E, Ramirez de Cartagena F, Pellicer N,
671 Tresserras J, Mutjé P. Modeling of the Tensile Moduli of Mechanical,
672 Thermomechanical, and Chemi-thermomechanical Pulps from Orange Tree Pruning.
673 Polymer Composites 2013; 1-7.
674 [34] Sharmin N, Khan RA, Salmieri S, Dussault D, Lacroix M. Fabrication and
675 Characterization of Biodegradable Composite Films Made of Using Poly(caprolactone)
676 Reinforced with Chitosan. Journal of Polymer Environmental 2012; 20:698–705.
677 [35] Di Franco CR, Busalmen JP, Ruseckaite RA, Vázquez A. Degradation of
678 Polycaprolactone/starch blends and composites with sisal fibre. Polymer Degradation
679 and Stability 2004; 86:95-103.
680 [36] Fortunati E, Armentano I, Zhou Q, Iannoni A, Saino E, Visai L, Berglund LA,
681 Kenny JM. Multifunctional bionanocomposite films of poly(lactic acid), cellulose
682 nanocrystals and silver nanoparticles. Carbohydrate Polymers 2012; 87:1596-1605.
683 [37] España, JM., Smaper, MD., Fages, E., Sánchez, LN, Balart, R. Investigation of the
684 Effect of Different Silane Coupling Agents on Mechanical Performance of Basalt Fiber
685 Composite Laminates with Biobased Epoxy Matrices. Polymer composites 2013: 376-
686 381.
687 [38] Sanchez-Garcia MD, Gimenez E, Lagaron JM. Morphology and barrier properties
688 of solvent cast composites of thermoplastic biopolymers and purified cellulose fibers.
689 Carbohydrate Polymers, 2008; 71(2): 235–244.

690 [39] Fukushima K, Tabuani D, Abbate C, Arena M, Rizzarelli P. Preparation,
691 characterization and biodegradation of biopolymer nanocomposites based on fumed
692 silica. European Polymer Journal 2011; 47:139–152.
693 [40] Chun KS, Husseinsyah S, Osman H. Modified Cocoa Pod Husk-Filled
694 Polypropilene Composites by using Methacrylic Acid. BioResources 2013; 8 (3): 3260-
695 3275.
696 [41] Valdés A, Beltrán, A, Garrigós, MC. Characterization and Classification of
697 Almond Cultivars by Using Spectroscopic and Thermal Techniques. Journal of Food
698 Science 2013; 78 (2):C138-C144.
699 [42] Jiménez A, Ruseckaite R. Binary mixtures based on polycaprolactone and cellulose
700 derivatives. Journal of Thermal Analysis and Calorimetry 2007; 88(3):851-6.
701 [43] Ruseckaite RA, Jiménez A. Thermal degradation of mixtures of polycaprolactone
702 with cellulose derivatives. Polymer Degradation and Stability 2003; 81(2):353-8.
703 [44] Dufresne,A, Vignon, M. Improvement of Starch Film Performances Using
704 Cellulose Microfibrils. Macromolecules 1998; 31: 2693-2696.
705 [45] Anglés, N, Dufrense, A. Plasticized Starch/Tunicin Whiskers Nanocomposites. 1.
706 Structural Analysis. Macromolecules 2000; 33: 8344-8353.
707 [46] Fukushima K, Abbate C, Tabuani D, Gennari M, Rizzarelli P, Camino G.
708 Biodegradation trend of poly (ε-caprolactone) and nanocomposites. Materials Science
709 and Engineering 2010; C 30:566-574.
710 [47] Chouzouri G, Xanthos M. Degradation of aliphatic polyesters in the presence of
711 inorganic fillers. Journal of Plastic Film & Sheeting 2007; 23: 19-36.
712

713 **Figure Captions.**

714 **Fig. 1**. Scanning electron micrographs of the fractured surface of PCL/AS composites
715 (500x).

716 **Fig. 2.** ATR-FTIR spectra obtained for AS residue, neat PCL (——) and PCL30%
717 composite (——).

718 **Fig. 3**. Water absorption curves obtained for neat PCL and PCL/AS composites as a
719 function of time (n=3; 23 ºC, 50 % RH).

720 **Fig. 4**. Melting (**a**) and crystallization (**b**) thermograms of neat PCL and PCL/AS
721 composite films, second heating.

722 **Fig. 5**. DTG curves obtained for AS residue, neat PCL and PCL/AS composites in nitrogen.

723 **Fig. 6**. Physical disintegration of PCL and PCL/AS composite films after 0, 30 and 75
724 days of disintegration in composting conditions at 25 ºC.

725 **Fig. 7.** Disintegrability (%) of neat PCL and PCL/AS composite films as a function of
726 degradation time in composting conditions at 25 ºC (n=2).

727 **Fig. 8.** DSC thermograms of PCL and PCL/AS composites at 0, 15, 30 and 75 days of
728 degradation in compost, second heating.

729 **Fig. 9.** Crystallization enthalpy values (ΔH_c) of neat PCL and PCL/AS composite films
730 as a function of degradation time in composting conditions at 25 ºC (n=2).

731

732 **Table 1**. Main significant FTIR bands observed for PCL and PCL/AS composites.

Band (cm^{-1})	Structural group
3450	O–H stretching vibrations of hydroxyl groups
2943	Symmetric C-H stretching vibrations
2866	Asymmetric C-H stretching vibrations
1724	C=O lactones stretching
1470	Asymmetric COO- stretching
1365	Symmetric COO- stretching and O-H bending
1180	C-O lactones stretching
1045	C-O-C stretching

733

734

735 **Table 2.** Mechanical (mean ± SD, n = 5) and barrier properties (mean ± SD, n = 3)
736 obtained for neat PCL and PCL/AS composites. Different superscripts within the same
737 row indicate statistically significant different values ($p < 0.05$).

Parameter	Formulation			
	PCL	PCL 10%	PCL 20%	PCL 30%
Elastic Modulus (MPa)	335 ± 8^{a}	392 ± 8^{b}	365 ± 4^{c}	280 ± 4^{d}
Elongation at break (%)	68 ± 7^{a}	38 ± 1^{b}	24 ± 1^{c}	18 ± 1^{d}
OTR.e ($cm^3 mm\ m^{-2}$ day)	90 ± 11^{a}	173 ± 8^{b}	160 ± 10^{b}	554 ± 20^{c}
WVP x 10^{-14} (Kg m $Pa^{-1}s^{-1}m^{-2}$)	2.5 ± 0.5^{a}	2.2 ± 0.1^{a}	3.1 ± 0.7^{b}	3.2 ± 0.3^{c}

738

739

740 **Table 3.** Thermal properties (mean ± SD, n = 3) obtained for neat PCL and PCL/AS
741 composites. Different superscripts within the same column indicate statistically
742 significant different values ($p < 0.05$).

Formulation	ΔH_c ($J\ g^{-1}$)	T_c (ºC)	ΔH_m ($J\ g^{-1}$)	T_m (ºC)	χ_c (%)	T_g (ºC)	T_{ini} (ºC)	T_{max} (ºC)
Control	59 ± 1^a	30 ± 1^a	59 ± 1^a	55 ± 1^a	43 ± 1^a	-61 ± 2^a	385 ± 2^a	415 ± 1^a
PCL 10%	55 ± 5^a	30 ± 1^a	55 ± 6^a	55 ± 1^a	45 ± 5^a	-60 ± 1^a	381 ± 2^a	415 ± 1^a
PCL 20%	57 ± 2^a	32 ± 1^b	54 ± 2^a	55 ± 1^a	50 ± 2^a	-57 ± 1^b	292 ± 7^b	411 ± 3^b
PCL 30%	54 ± 1^b	33 ± 1^b	44 ± 1^b	44 ± 1^b	46 ± 1^b	-56 ± 1^b	272 ± 5^c	404 ± 5^c

743

744

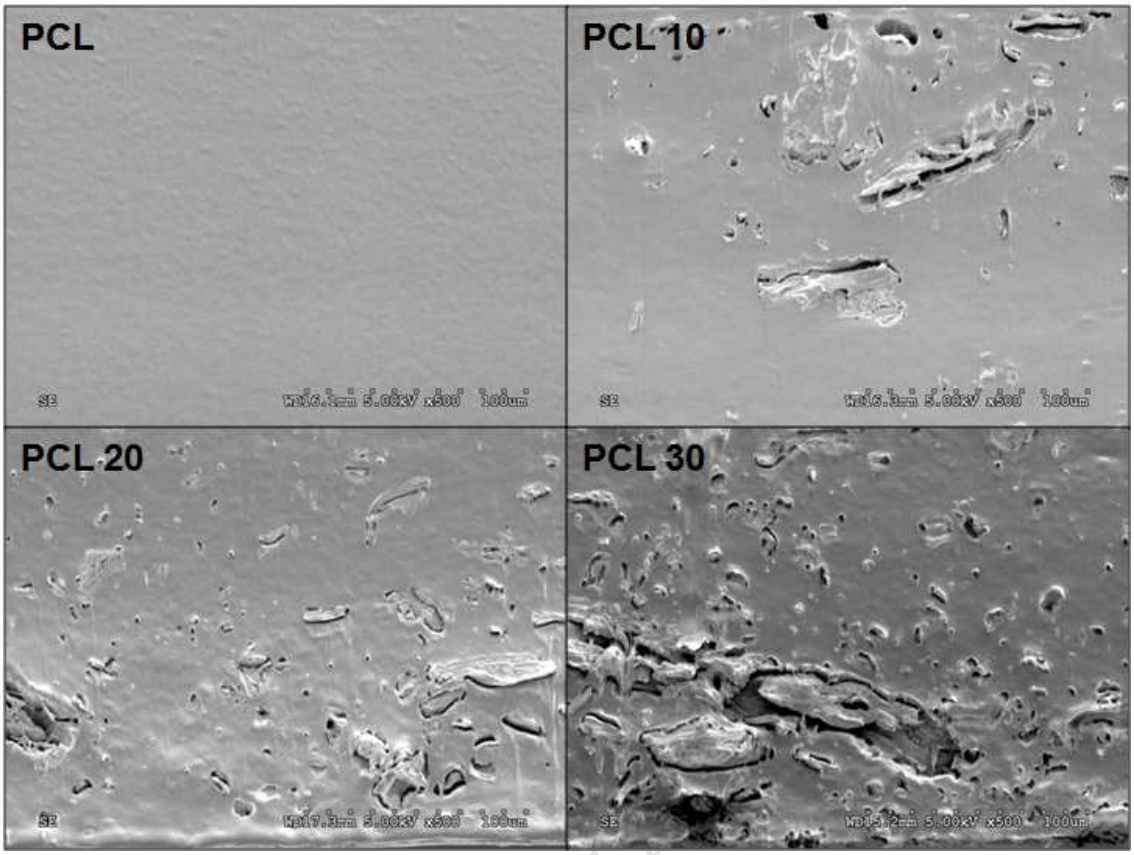

745

746 **Fig. 1.** Scanning electron micrographs of the fractured surface of PCL/AS composites

747 (500x).

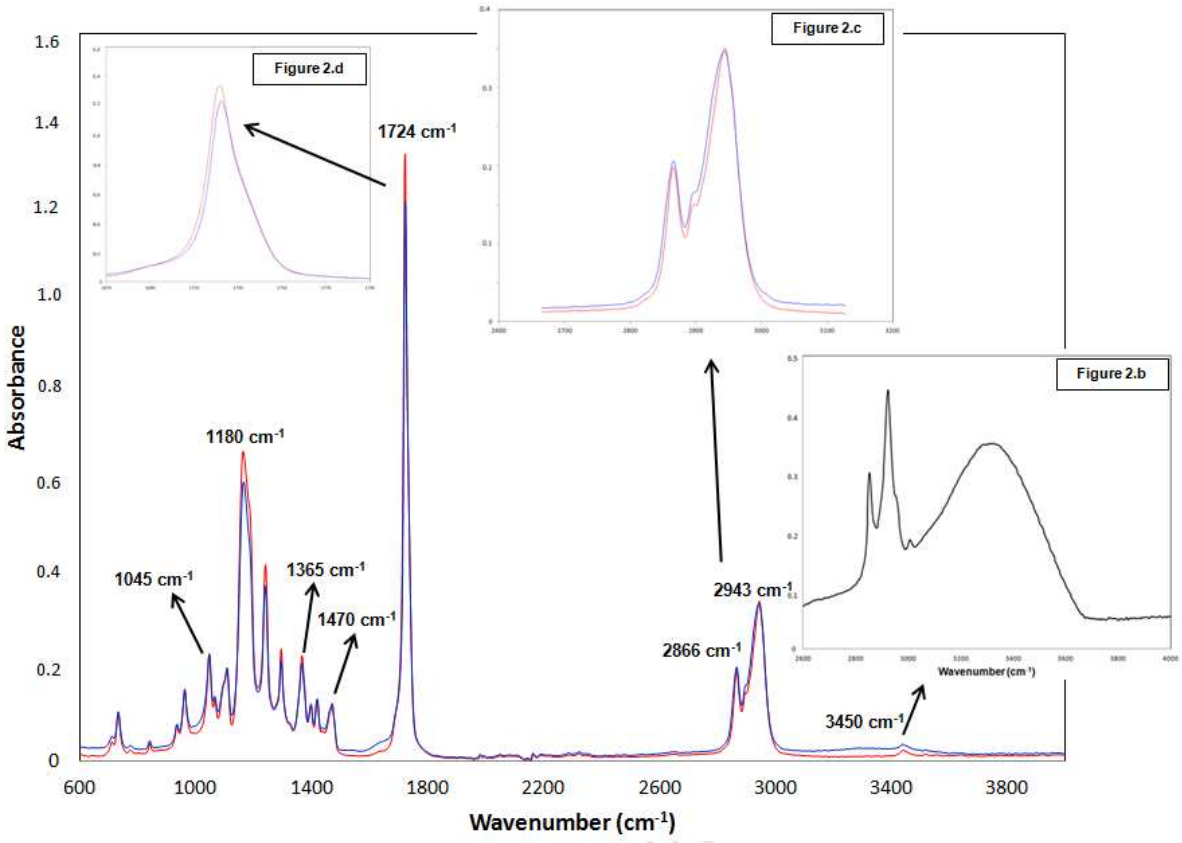

748

749 **Fig. 2.** ATR-FTIR spectra obtained for AS residue, neat PCL (——) and PCL30%

750 composite (——).

751

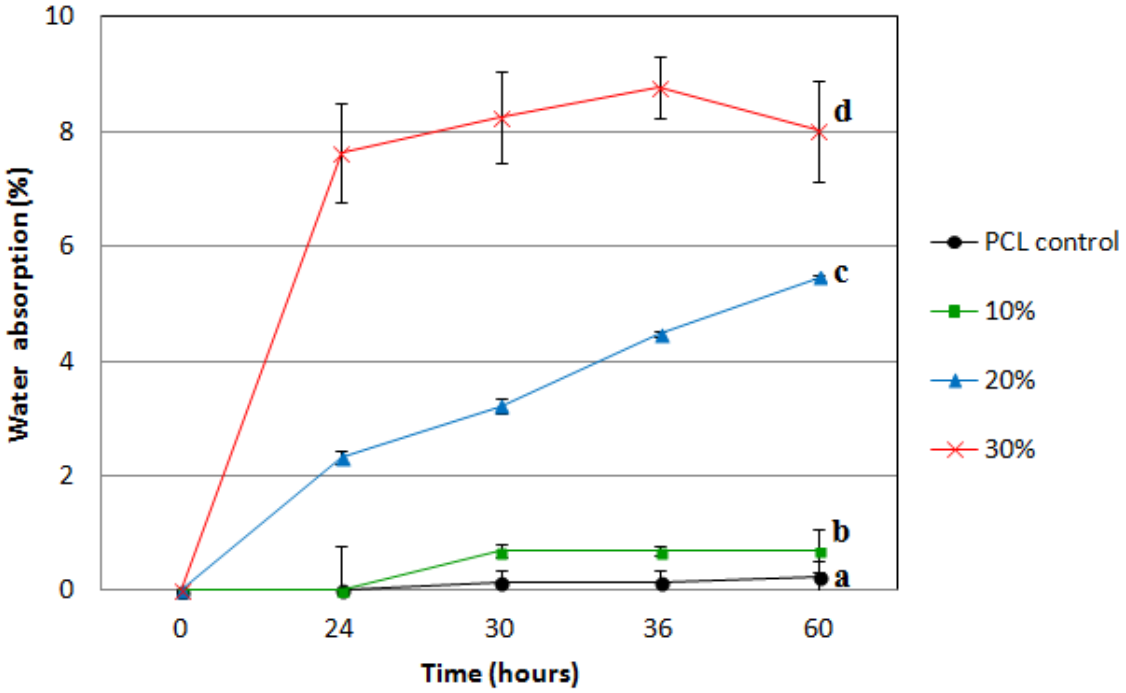

752

753 **Fig. 3.** Water absorption curves obtained for neat PCL and PCL/AS composites as a

754 function of time (n=3; 23 ºC, 50 % RH).

755

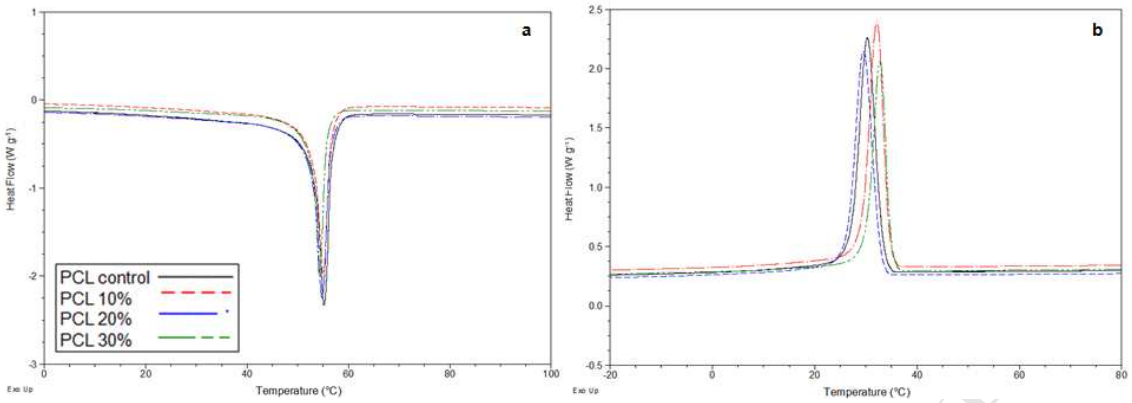

Fig. 4. Melting (**a**) and crystallization (**b**) thermograms of neat PCL and PCL/AS composite films, second heating.

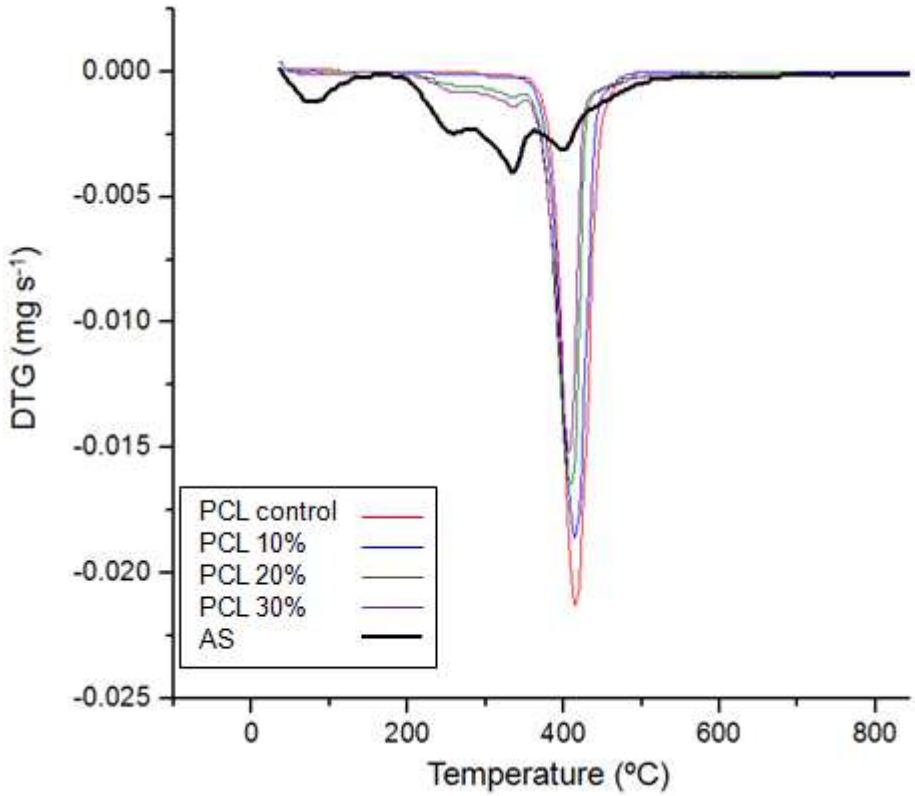

760

761 **Fig. 5.** DTG curves obtained for AS residue, neat PCL and PCL/AS composites in

762 nitrogen.

763

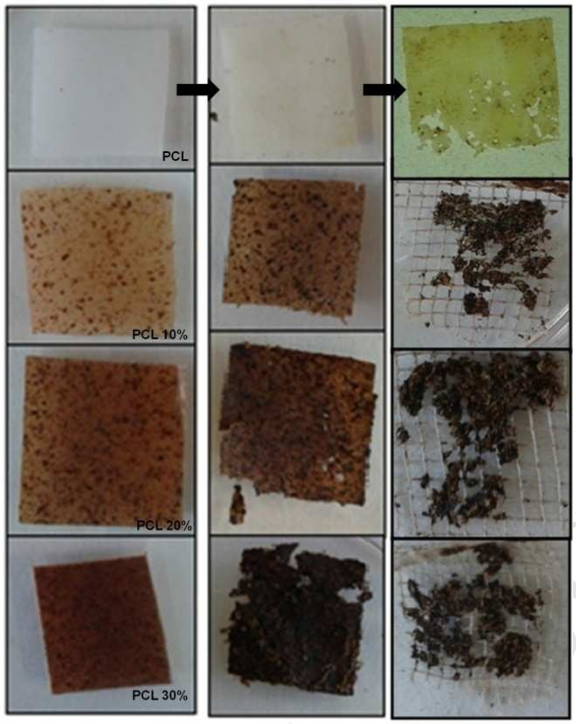

764

765 **Fig. 6.** Physical disintegration of PCL and PCL/AS composite films after 0, 30 and 75

766 days of disintegration in composting conditions at 25 ºC.

767

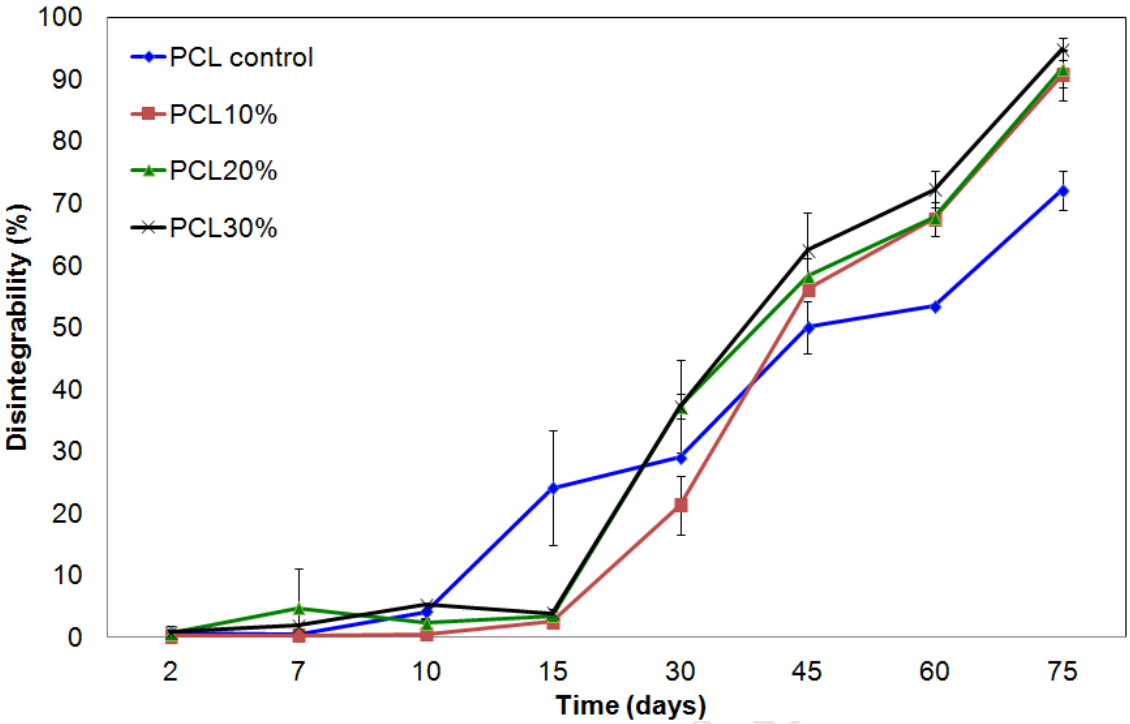

768

769 **Fig. 7.** Disintegrability (%) of neat PCL and PCL/AS composite films as a function of

770 degradation time in composting conditions at 25 ºC (n=2).

771

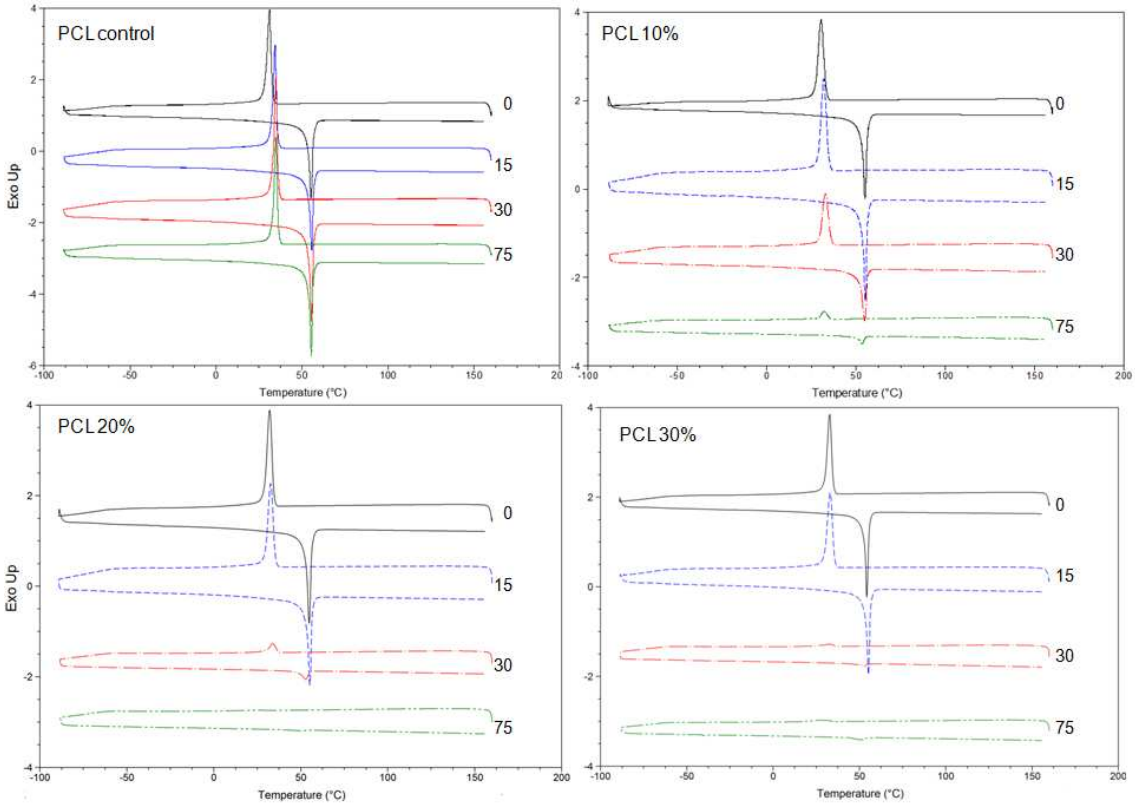

772

773 **Fig. 8.** DSC thermograms of PCL and PCL/AS composites at 0, 15, 30 and 75 days of

774 degradation in compost, second heating.

775

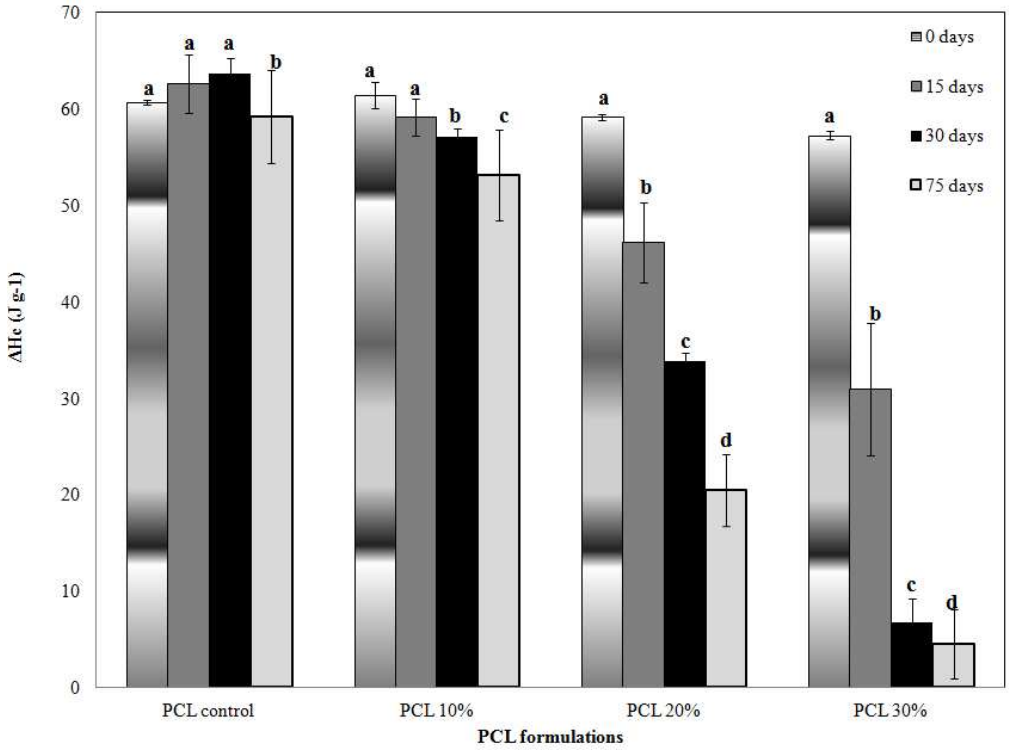

776

777 **Fig. 9.** Crystallization enthalpy values (ΔH_c) of neat PCL and PCL/AS composite films

778 as a function of degradation time in composting conditions at 25 ºC (n=2).